Induction-Coil Measurement System for Normal- and Superconducting Solenoids

Carlo Petrone, Stefano Sorti, Eivind Dalane, Bertrand Mehl, and Stephan Russenschuck

***Abstract*—The magnetic measurement of solenoids relies on different methods to characterize the field quality and locate the magnetic axis. Usually, Hall mappers and stretched-wire systems are used for these tasks. This paper presents an alternative, fluxmetric method to measure the radial field dependence and the magnetic axis with a single instrument. The solenoidal-field transducer is based on a disc-shaped induction-coil array with concentric coils and 90 deg. arc segments mounted on a translation stage. This allows to sample the magnet along its axis and to extract both the longitudinal and transversal field components. The design, development, and validation of the new instrument are described. The induction coil, which is the core of this instrument, is fabricated in printed-circuit board technology, which has become the new standard for these applications. Results of recent measurements of a normal-conducting solenoid magnet are given.**

***Index Terms*—Superconducting magnets, solenoids, measurements and techniques, materials testing.**

I. Introduction

The High-Luminosity Large Hadron Collider (HL-LHC) accelerator project [1] raised new challenges for measuring and aligning the magnetic axis. For long, straight accelerator magnets, the measured quantities are typically the field integrals, because they obey the regularity conditions of the two-dimensional field distributions in simply connected domains [2]. In this case, the magnetic flux density can be expressed as a Fourier series, with coefficients know as field harmonics or multipoles [3]. The alignment of the solenoid assembly is demanding and requires dedicated tools and iterative processes. Projects such as the Hollow Electron Lens (HEL) [4], [5] and Electron Cooler [6] required us to develop a different approach for expressing the local flux-density distribution for measuring the axis and aligning the solenoids by the transverse field components at the fringe-field zones. Following previous experience [7], we propose a method to locate the magnetic axis of solenoids, employing a translating induction-coil magnetometer that is displaced in the bore of a normal-conducting magnet, or within an anticryostat in the case of a superconducting magnet tested at crygoenic temperatures. The method retrieves all the magnet properties (longitudinal and transverse field distribution, as well as the magnetic axis) from a single transducer, avoiding the combination of methods based on Hall probes [8], laser compass [9] and vibrating wires [10]. Moreover, and in contrast to Hall-probe measurement systems, the proposed method features a linear response for the longitudinal and radial field components.

Manuscript received November 30, 2021; revised January 16, 2022; accepted January 18, 2022. Date of publication January 31, 2022; date of current version March 11, 2022. *(Corresponding author: Carlo Petrone.)*

The authors are with CERN, 1217 Geneva, Switzerland (e-mail: carlo.petrone@cern.ch).

Color versions of one or more figures in this article are available at https://doi.org/10.1109/TASC.2022.3147142.

Digital Object Identifier 10.1109/TASC.2022.3147142

II. The Measurement Principle

Solving a boundary value problem in spherical coordinates (R, ϑ, φ) will provide us with a multipole expression for solenoids when assuming axial symmetry, that is, $\partial\phi_\mathrm{m}/\partial\varphi = 0$. The general solution for the magnetic scalar potential inside a sphere, free of any current sources and magnetic material, can then be written as [2]

$$\phi_\mathrm{m}(R,\vartheta) = \sum_{n=0}^{\infty} \mathcal{A}_n R^n P_n(\cos\vartheta). \tag{1}$$

In this context, the functions $P_n(\cos\vartheta)$ are called *zonal spherical functions* or *zonal harmonics*. The $\mathcal{A}_n$ are yet unknown coefficients that must be extracted from the measurements. For differentials of the Legendre polynomials, one finds the recurrence relation

$$\frac{\mathrm{d}P_n(x)}{\mathrm{d}x} = \frac{n}{x^2-1}\left(xP_n(x) - P_{n-1}(x)\right). \tag{2}$$

From the magnetic scalar potential, we can calculate the components of the magnetic flux density by

$$B_R = -\mu_0 \sum_{n=1}^{\infty} \mathcal{A}_n n R^{n-1} P_n(\cos\vartheta), \tag{3}$$

$$B_\vartheta = \mu_0 \sum_{n=1}^{\infty} \mathcal{A}_n R^{n-1}\, P_n^1(\cos\vartheta), \tag{4}$$

where P_n^1 are the *associated Legendre polynomials* of order n and degree 1;

$$P_n^1(\cos\vartheta) = -\sin\vartheta \frac{\mathrm{d}P_n(\cos\vartheta)}{\mathrm{d}\cos\vartheta} = \frac{\mathrm{d}P_n(\cos\vartheta)}{\mathrm{d}\vartheta}. \tag{5}$$

For differentials of the associated Legendre polynomials it yields

$$\frac{\mathrm{d}P_n^m(x)}{\mathrm{d}x} = \frac{1}{x^2-1}\left(nxP_n(x) - (n+m)P_{n-1}^m(x)\right). \tag{6}$$

The multipole coefficients $\mathcal{A}_n$ are not determined at this stage. They are defined by the boundary conditions at some reference radius R_0 or can be calculated from the Legendre series expansion of the simulated or measured radial component of the magnetic flux density at R_0.

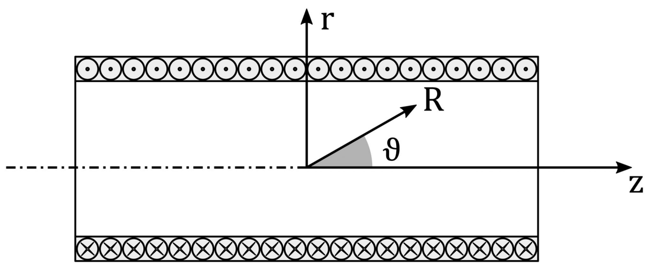

Fig. 1. Coordinate systems for axisymmetric solenoid.

A cylindrical coordinate system (r, φ, z) is now introduced where z is the solenoid axis; see Fig. 1. The B_z and B_r components of the magnetic flux density can be expressed in terms of R and ϑ as

$$B_z(R, \vartheta) = B_R \cos\vartheta - B_\vartheta \sin\vartheta, \tag{7}$$

$$B_r(R, \vartheta) = B_R \sin\vartheta + B_\vartheta \cos\vartheta\,; \tag{8}$$

Using the Legendre series (3) and (4) we get

$$B_z(R, \vartheta) = -\mu_0 \sum_{n=1}^{\infty} \mathcal{A}_n\, n\, R^{n-1}\, P_{n-1}(\cos\vartheta), \tag{9}$$

$$B_r(R, \vartheta) = \mu_0 \sum_{n=1}^{\infty} \mathcal{A}_n\, R^{n-1}\, P^1_{n-1}(\cos\vartheta). \tag{10}$$

For the calculation of the multipole coefficients we expand the field into a Taylor series about z_0:

$$B_z(z) = \sum_{n=0}^{\infty} \frac{1}{n!} B_z^{(n)}(z_0)(z - z_0)^n, \qquad z - z_0 < R_0, \tag{11}$$

where $B_z^{(n)}(z_0) := \frac{\mathrm{d}^n B_z(r=0)}{\mathrm{d}z^n}|_{z=z_0}$. The solution (9) reduces for $\vartheta = 0$, $z - z_0 = R > 0$, and $P_n(1) = 1$ to

$$B_z(z) = -\mu_0 \sum_{n=1}^{\infty} \mathcal{A}_n n (z - z_0)^{n-1} \tag{12}$$

and therefore

$$\mathcal{A}_n = \frac{-B_z^{(n-1)}(z_0)}{\mu_0\, n\, (n-1)!}. \tag{13}$$

The components of the magnetic flux density at an arbitrary point inside the sphere $R < R_0$ can then be calculated with Eqs. (9) and (10). For the B_r component, this yields with $R = r$ and $\vartheta = \pi/2$:

$$\begin{aligned} B_r(r, z_0) &= \mu_0 \left(r\mathcal{A}_2 - \frac{3}{2} r^3 \mathcal{A}_4 - \cdots \right) \\ &= -\frac{r}{2}\, \frac{\mathrm{d}B_z(0,z)}{\mathrm{d}z}\bigg|_{z_0} + \frac{r^3}{16}\, \frac{\mathrm{d}^3 B_z(0,z)}{\mathrm{d}z^3}\bigg|_{z_0} - \cdots . \end{aligned} \tag{14}$$

A similar expression can be derived for $B_z(r, z_0)$ from (12).

III. The Measurement Procedure

The field transducer comprises two sets of induction coils. As shown in Fig. 2, the first set of coils (D_i) consists of five nested circular disks, while the second set consists of 4×4 arcs of 90 degrees opening angle ($\mathrm{Q}_{q,j}$) where r_i are the radii of the outermost wire turn of the disks, while r_j are the barycenters of the arcs. The disks are numbered from inside out ($i \in [1, 5]$), while the quarter arcs are numbered with the first index (q) denoting the quadrant (clockwise) and the second (j) the radius from inside out. When the measurement system is displaced in the longitudinal direction in the magnetic bore, along the z-axis, the induced voltages across the coils are acquired "on the fly". The position of the induction coil can be identified as $\boldsymbol{r}_\mathrm{c} = (r_\mathrm{c}, \varphi_\mathrm{c}, z_\mathrm{c})$. Considering the longitudinal position z_c as a precisely known parameter, determined by the longitudinal displacement system of the sensor, the average flux density across the induction coils can be expanded up to 5^{th} order as

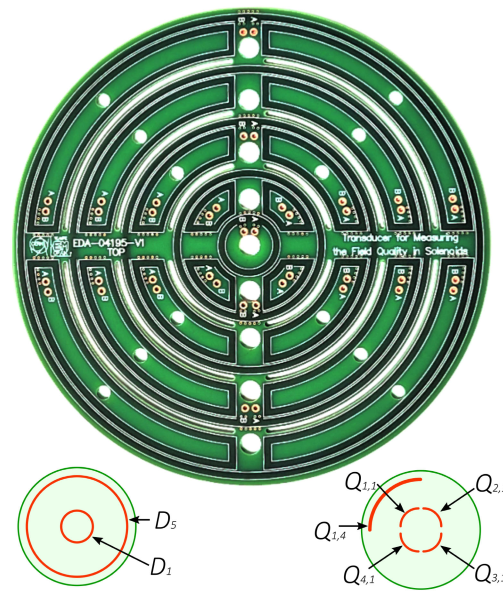

Fig. 2. PCB layout and naming convention for disks ($\mathrm{D}_i, i \in [1, 5]$ from inside out) and quarter-arc coils ($\mathrm{Q}_{q,j}, q \in [1, 4]$ clockwise, $j \in [1, 4]$ from inside out).

$$\begin{aligned} B_z(r) &= p_0(z_\mathrm{c}) + p_2(z_\mathrm{c})\, r^2 + p_4(z_\mathrm{c})\, r^4 + \cdots \\ B_r(r) &= q_1(z_\mathrm{c})\, r + q_3(z_\mathrm{c})\, r^3 + q_5(z_\mathrm{c})\, r^5 + \cdots \end{aligned} \tag{15}$$

where the p_n and q_n are the Taylor coefficients to be determined. These coefficients, which are functions of z_c, can be deduced from the field harmonics in (14) and vice-versa.

A. Measuring the Field Components

The average axial field through each circular coil can be computed as $\bar{B}_{z,i}(z_k) = \phi_i(z_k)/S_i$, where $\phi_i(z_k)$ is the flux linkage of the coil at a given longitudinal position $z_k, k \in [1, K]$, where K is the total number of trigger points for the linear encoder travel range. S_i is the coil surface measured in m^2 and calibrated in a pure dipole field. The radial dependence of the flux density can be deduced from the measurements by subtracting the flux linkages of two concentric disks [7]. For measuring the absolute field strength at a position z_k, the induction coils must be moved from the zero-field region outside of the magnet, such that $\bar{B}_{z,i}(z_0) = 0$.

The radial field component is deduced from the rate of change of flux divided by the cylinder surface traced by each disk edge

TABLE I
THE CALIBRATED COIL SURFACE AND RADIUS VALUES TOGETHER WITH THE RESISTANCE OF THE COILS

Coil	D_1	D_2	D_3	D_4	D_5	$Q_{1,1}$	$Q_{1,2}$	$Q_{1,3}$	$Q_{1,4}$	$Q_{2,1}$	$Q_{2,2}$
S [m^2]	0.0051	0.0356	0.1063	0.2145	0.3605	0.0026	0.0073	0.0121	0.0168	0.0026	0.0073
r [mm]	5	14	24	34	44	10	20	30	40	10	20
R [Ω]	22.83	42.54	66.07	91	114.45	20.29	32.27	44.21	56.43	20.07	31.84
Coil	$Q_{2,3}$	$Q_{2,4}$	$Q_{3,1}$	$Q_{3,2}$	$Q_{3,3}$	$Q_{3,4}$	$Q_{4,1}$	$Q_{4,2}$	$Q_{4,3}$	$Q_{4.4}$	
S [m^2]	0.0121	0.0168	0.0026	0.0073	0.0121	0.0168	0.0026	0.0073	0.0121	0.0168	
r [mm]	30	40	10	20	30	40	10	20	30	40	
R [Ω]	44.02	55.34	20.19	32.03	44.27	55.76	19.70	32.18	43.91	55.98	

during the longitudinal displacement:

$$\bar{B}_{r,i}(z_k) = \frac{\phi_i(z_k) - \phi_i(z_{k-1})}{2\pi r_i\ (z_k - z_{k-1})N}, \tag{16}$$

where N is the number of coil turns ($N = 60$), and $(z_k - z_{k-1})$ is the longitudinal displacement step.

B. Magnetic Axis Location

The quarter-arc coils $Q_{q,j}$ of the sensor can be employed to locate the magnetic axis of the solenoid with respect to the mechanical center of the field sensor. At every trigger point z_k, 16 signals are acquired. Using the expansion of $B_z(r)$ as in (15), the location of magnetic axis can be computed. To simplify the measurement post-processing we consider that

- the winding thickness of the arc-segment coil is much smaller than their circumference;
- there is only a small misalignment between the center of the sensor and the magnetic axis, and therefore the radial component of the magnetic flux density is approximately constant along each arc;
- the tilt and swing angles of the sensor can be neglected, assuming the sensor is moving perpendicularly to the longitudinal axis.

In this way, each arc segment can be assigned an average flux density $\bar{B}_{k,q,j}$ at its barycenter with the position vector in the magnet frame $\boldsymbol{r}_{k,q,j} = (R_{q,j}, \varphi_{q,j}, z_k)$. The center of the field sensor is located at $\boldsymbol{r}_\mathrm{c} = (r_\mathrm{c}, \varphi_\mathrm{c}, z_k)$ in the magnet frame. Owing to the assumption that the tilt and swing angles can be neglected, the parameters to be fitted are: $p_0(z_k)$, $p_2(z_k)$, $p_4(z_k)$, r_c and φ_c.

Consider now that the measured quantities are the local gradients of B_z averaged over the surfaces of the quarter arcs: $\bar{g}(\boldsymbol{r}) := \mathrm{grad}_{\boldsymbol{r}} \boldsymbol{B} \cdot \boldsymbol{e}_z$ for all $\boldsymbol{r} = \boldsymbol{r}_{q,j,k} = (R_{q,j}, \varphi_{q,j}, z_k)$. These signals are then fitted with the expression in (15). The magnetic axis is found where the local field gradient takes its minimum. For this root-finding problem it is beneficial to consider the points z_c where the signal-to-noise ratio is maximal. This is the case at the extremities of the solenoid.

IV. MEASUREMENT RESULTS

The sensor has been employed in the measurement of a normal-conducting solenoid. The magnet (PXML-BA-WC) is 390 mm long, and has an aperture of 180 mm. For a nominal current of 700 A, the peak field in the center of the magnet is about 0.46 T.

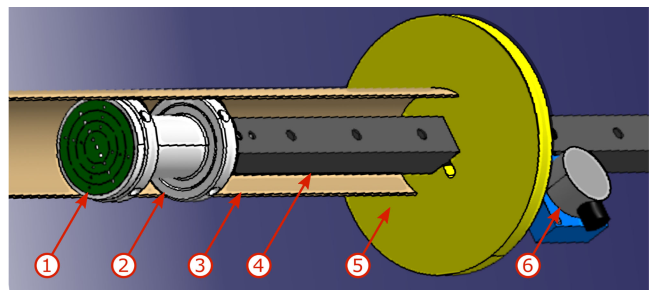

Fig. 3. Measurement system layout: (1) PCB coils, (2) Teflon PCB support and sledge, (3) guidance tube, (4) supporting arm, (5) anti-cryostat fixing plate, (6) linear encoder head.

A. The Measurement Setup

Fig. 3 shows schematically the field transducer, originally designed and developed for measuring a 9 T superconducting magnet. Table I gives the coil surfaces S, radii r, and ohmic resistance R of the field transducer (featuring ten active layers), which is moved along the magnet axis on a sled. For magnets with low field levels, the measurement sensitivity can be adjusted by increasing the coil surfaces S, i.e., increasing the number of layers in the PCB board. For measuring the field homogeneity in the central part of the magnet bore, the flux linkages with the disks are referenced to the positions measured with a linear encoder. A wire-draw encoder (SICK PFG08-P1AM03PP) is used to measure the probe's distance to an end plate and trigger the signal-acquisition system, comprising a digital integrator (FDI) [11]. A number of runs per direction are recorded, and the signals are averaged. A travel range of 2.5 m is sufficient to cover the field region of the solenoid. The encoder guarantees a maximum resolution of 0.014 mm, even though the triggers are set to 0.11 mm. The Leica laser system (Absolute Tracker AT960, with a tracking accuracy of 10 μ m) is employed to validate the accuracy of the encoder. For a 250 mm displacement, the relative error of the encoder is about 0.25 mm (0.1%), which can amount to 3 mm over the entire travel range. As the encoder is relative, the absolute reference must be taken mechanically at the end plate. The Leica laser system could also be used directly

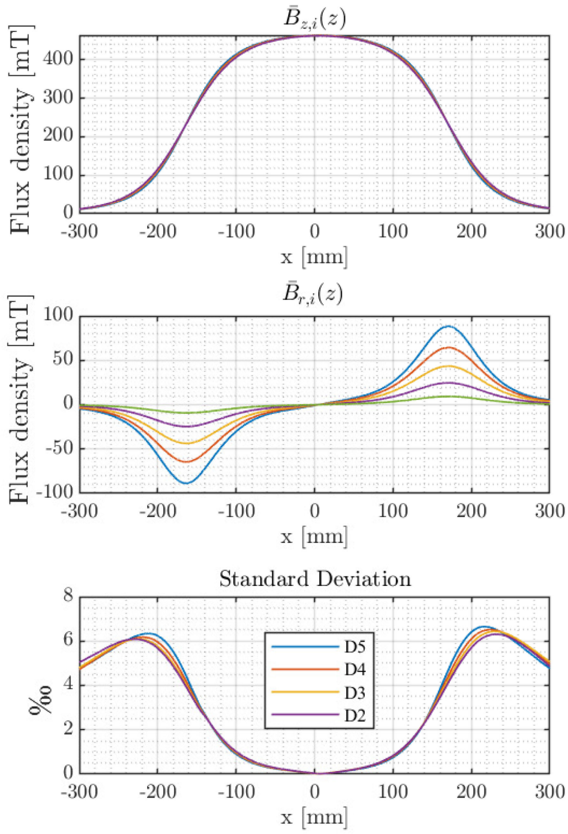

Fig. 4. Flux density $\bar{B}_{z,i}(z)$ (top) and $\bar{B}_{r,i}(z)$ (middle) extracted from the 5 main disks averaged over 6 consecutive runs, and standard deviation over 6 measurement runs (bottom).

as a triggering system if a better longitudinal position reference was required.

B. The B_z and B_r Field Distribution

Fig. 4 shows the results of the longitudinal and transversal field components as a function of the longitudinal position. To study the measurement precision 6 consecutive runs were used to evaluate the measurement standard deviation. Despite the relatively low magnitude of the field, for which the sensor surfaces were not optimized, the repeatability of the measurement is at the 10^{-4} level in the centre of the solenoid, degrading to about 2×10^{-3} at the solenoid extremities (at ± 150 mm), as shown in Fig. 4 (bottom). The disks D_2, D_3, D_4, and D_5, reach a maximum deviation of about 5×10^{-3} at the solenoid extremities, while the Disk 1 is reported being not sufficiently sensitive due to the smallest active area (see Table I). The repeatability of the measurement is mainly limited by the repeatability of the longitudinal triggering system, which can easily be improved if required, for example, by mounting the sensor on a precision alignment stage or using an optical interferometer to trigger the acquisition.

C. Magnetic Axis Localization

In order to validate the proposed method for the axis location, measurements were taken along nine tracks, shifted on the horizontal plane in parallel to the geometric axis, by $-20, -15, -10, -5, 0, 5, 10, 15, 20$ mm. The positions were precisely measured with the laser tracker. For every track, the measurements were averaged over 6 travel repetitions.

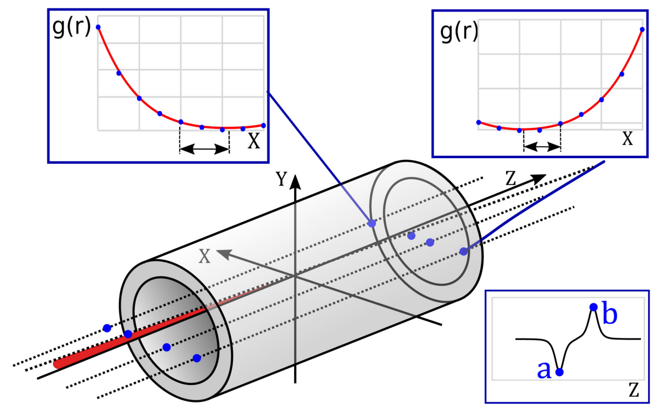

Fig. 5. Principle of the magnetic axis localization, moving the transducer on parallel tracks in the magnet bore. The two upper plots show the fit of the local field gradients, measured on the two outer tracks at the magnet extremity b.

The acquired signal has two peaks at the extremities of the solenoid; positions a and b shown in Fig. 5. At each position z_k, (15) is used to fit the local field gradients. At the longitudinal positions a and b, the resulting set of measured local gradients $\bar{g}(\boldsymbol{r})$ is used to evaluate the relative displacement of the track r_c. As shown in the Fig. 5, each measurement is fitted in its local reference frame and then transformed into the magnet frame.

The results show that with a single track the magnetic axis can be located with a precision of 0.1 mm. When all tracks are fitted, the axis location is within 50 μm when averaging the measured axes. A second measurement campaign was performed, deliberately imposing a swing-angle misalignment to the traveling axis within the horizontal plane of the magnet. The measurement results have shown a precision within 0.1 mrad in identifying this imposed swing angle.

V. Conclusion

The proposed method allows us to measure the field profiles of the B_z and B_r components with an accuracy of 10^{-5} with respect to the main field. The local field gradients were determined by moving the sensor along displaced tracks. This allowed the magnetic axis location with a precision of 0.1 (single track) and 0.05 mm (9 tracks), and 0.1 mrad for the swing angle. Proven the feasibility, a more accurate result may be expected by producing an optimized sensor for each particular project, by mounting the sensor on a precision alignment stage or using an optical interferometer to trigger the acquisition, and by removing the hypotheses in Section III-B. This could be accomplished by deriving an observation function that takes all the individual turns and shapes of the quarter-arc coils into account.

REFERENCES

[1] I. B. Alonso, O. Bruning, P. Fessia, L. Rossi, L. Tavian, and M. Zerlauth, "High-luminosity large hadron collider (HL-LHC): Technical design report," CERN, Geneva, Switzerland, Tech. Rep. FERMILAB-PUB-15-699-TD, 2020, doi: 10.23731/CYRM-2020-0010.

[2] S. Russenschuck, *Field Computation for Accelerator Magnets. Analytical and Numerical Methods for Electromagnetic Design and Optimization*. Weinheim, Germany: Wiley, 2010.

[3] S. Russenschuck, "Rotating- and translating-coil magnetometers for extracting pseudo-multipoles in accelerator magnets," *Int. J. Comput. Math. Elect. Electron. Eng.*, vol. 36, no. 5, pp. 1552–1567, 2017, doi: 10.1108/COMPEL-02-2017-0059.

[4] G. Stancari *et al.*, "Conceptual design of hollow electron lenses for beam halo control in the large hadron collider," Geneva, Switzerland, Tech. Rep. FERMILAB-TM-2572-APC, CERN-ACC-2014-0248, CERN, 2014.

[5] D. Perini, A. Kolhemainen, A. Rossi, S. Sadovich, and G. Stancari, "Design of high-performance guns for the HL-LHC HEL," *J. Instrum.*, vol. 16, Mar. 2021, Art. no. T03010.

[6] D. Tommasini, "New AD electron cooler: Kick-off meeting." [Online]. Available: https://indico.cern.ch/event/962591/

[7] C. Petrone, B. Bordini, M. Buzio, and S. Russenschuck, "A transducer for measuring the field quality in superconducting solenoids," *IEEE Trans. Appl. Supercond.*, vol. 30, no. 4, Jun. 2020, Art no. 9000505, doi: 10.1109/TASC.2020.2971446.

[8] K. H. Park *et al.*, "Field mapping system for solenoid magnet," *Proc. AIP Conf. Proc.*, 2007, vol. 879, pp. 260–263. [Online]. Available: https://doi.org/10.1063/1.2436051

[9] V. N. Bocharov, A. V. Bublei, S. G. Konstantinov, V. M. Panasyuk, and V. V. Parkhomchuk, "Precision measurements and compensation for the transverse components of the solenoids' magnetic field," *Instrum. Exp. Techn.*, vol. 48, no. 6, pp. 772–779, 2005. [Online]. Available: https://doi.org/10.1007/s10786-005-0139-2

[10] P. Arpaia, C. Petrone, S. Russenschuck, and L. Walckiers, "Vibrating-wire measurement method for centering and alignment of solenoids," *J. Instrum.*, vol. 8, 2013, Art. no. P11006, doi: 10.1088/1748-0221/8/11/P11006.

[11] P. Arpaia *et al.*, "A fast digital integrator for magnetic field measurements at CERN," in *Proc. IEEE Instrum. Meas. Technol. Conf.*, 2006, pp. 67–71, doi: 10.1109/IMTC.2006.328175.